Interactions of fast ions with carbon nanotubes: Self-energy and stopping power

You-Nian Wang*
The State Key Laboratory of Materials Modification, Department of Physics, Dalian University of Technology, Dalian 116023, People's Republic of China

Z. L. Mišković
Department of Applied Mathematics, University of Waterloo, Waterloo, Ontario, Canada N2L 3G1
(Received 21 August 2003; published 3 February 2004)

The interactions of charged particles with carbon nanotubes are studied by means of the linearized hydrodynamic theory for electronic excitations on the nanotube surface. General expressions are derived for the induced potential, the self-energy, and the stopping power for a charged particle moving paraxially in a nanotube. Numerical results are obtained showing the influence of the damping factor, the nanotube radius, and the particle position on its self-energy and the stopping power. Results for stopping power in the linearized hydrodynamic model are compared with those obtained by means of the dielectric formalism in random-phase approximation, showing a close agreement between the two approaches for high speeds of charged particles.

DOI: 10.1103/PhysRevA.69.022901 PACS number(s): 79.20.Rf, 34.50.Bw, 34.50.Dy

I. INTRODUCTION

Following the discovery of carbon nanotubes, there has been a growing interest in interactions of charged particles with the nanotubes, which may be relevant for applications in several areas of research and technology. For example, important information about the electronic structure of carbon nanotubes can be obtained using the electron probe techniques, such as the transmission-electron microscopy [1] and the electron energy-loss spectroscopy (EELS) [2,3]. In particular, in some of the most intriguing applications, it has been demonstrated that carbon nanotubes may be used to efficiently steer (deflect and focus) charged-particle beams [4–8], in the way quite similar to crystal channeling.

A powerful theoretical tool for studying such interactions is provided by the dielectric response formalism, which has been implemented in restricted geometries in a number of pioneering studies by Ritchie and co-workers [9]. During the past several years, significant progress has been achieved in theoretical study of transport, or channeling, of charged particles through microcapillaries and nanocapillaries in solids [10–14]. In particular, Arista *et al.* [12–14] have calculated recently the self-energy and the energy loss of charged particles moving through cylindrical channels, or cavities, in solids. It should be pointed out that the structures studied in all those reports contained solid regions characterized by the bulk dielectric functions for three-dimensional (3D) electron gas models, which were separated, or bounded, by cylindrical interfaces.

Carbon nanotubes present systems which are quite different from the cavities in solids or nanowires made of different materials. Although all these systems share the same underlying cylindrical geometry, carbon nanotubes cannot be modeled as a part of a 3D structure. Actually, elementary excitations on a nanotube may be modeled by an infinitesimally thin layer of quasi-free-electron gas, uniformly distributed over an infinitely long cylindrical surface of a tubule. At zero temperature, such a two-dimensional (2D) model of electron gas is completely parametrized by its surface density and the radius of the tubule. Important contribution in theoretical description of such structures has been recently reported by Stöckli *et al.* [15], who have deduced the dielectric properties of carbon nanotubes by means of the hydrodynamic theory of plasmon excitations in the 2D electron gas on a cylindrical surface, in order to interpret the EELS data for collective excitations on single-wall carbon nanotubes, caused by the incidence of fast electrons perpendicular to the nanotube. Very recently, we have used a dielectric formalism [16] to study the energy loss of charged particles moving parallel to the axis in cylindrical tubules. In that formalism, the elementary excitations of the electron gas are described by a dielectric function in the random-phase approximation (RPA), which depends on the angular momentum, the wave number, the frequency, and the tubule geometry [17].

In the present paper, we adopt and extend the hydrodynamic model [15] by including the single-electron excitations on nanotube surfaces, in order to study the self-energy and the energy loss of charged particles moving paraxially inside nanotubes. In particular, we wish to elucidate possible effects of the ion self-energy (akin to the image interaction with the walls of nanotubes) on ion trajectories in the proposed ion-channeling applications of carbon nanotubes [4–8]. As a secondary goal, the results presented here for ion stopping provide a possibility to compare the advantages of the hydrodynamic theory with those of the dielectric theory in RPA [16,17] in dealing with the energy losses in carbon nanotubes. Section II provides details of calculations of the self-energy and the stopping power in the hydrodynamic model, while a comparison of the stopping powers in the hydrodynamic and the RPA dielectric models is provided in Sec. III. Concluding remarks are given in Sec. IV. Atomic units (a.u.) are used throughout, unless otherwise indicated.

II. HYDRODYNAMIC THEORY

We model a single-wall carbon nanotube as an infinitesimally thin and infinitely long cylindrical shell with the radius

*Email address: ynwang@dlut.edu.cn

 ©2004 The American Physical Society

a, and assume that the valence electrons can be considered a free-electron gas distributed uniformly over the cylindrical surface, with the density per unit area n_0. We use cylindrical coordinates $\mathbf{r}=(\rho,\phi,z)$ and consider a charged particle with the charge Q, moving within the nanotube, with its trajectory parallel to the nanotube axis z, such that the particle's instantaneous position is given by $\mathbf{r}_0=(\rho_0,\phi_0,vt)$, where v is the particle's speed. The homogeneous electron gas will be perturbed by the charged particle and can be regarded as a charged fluid with the velocity field $\mathbf{u}(r_S,t)$ and the perturbed density (per unit area) $n_1(\mathbf{r}_S,t)$, where $\mathbf{r}_S=(\phi,z)$ are the coordinates of a point at the cylindrical surface of the nanotube. Note that the velocity field $\mathbf{u}$ has only tangential components to the nanotube surface. Based on the linearized hydrodynamic model [15], the electronic excitations on the cylindrical surface can be described by the continuity equation

$$\frac{\partial n_1(\mathbf{r}_S,t)}{\partial t}+n_0\boldsymbol{\nabla}_\parallel\cdot\mathbf{u}(r_S,t)=0, \tag{1}$$

the momentum-balance equation

$$\frac{\partial\mathbf{u}(\mathbf{r}_S,t)}{\partial t}=\boldsymbol{\nabla}_\parallel\Phi(\mathbf{r},t)\big|_{\rho=a}-\frac{\alpha}{n_0}\boldsymbol{\nabla}_\parallel n_1(\mathbf{r}_S,t)+\frac{\beta}{n_0}\boldsymbol{\nabla}_\parallel[\boldsymbol{\nabla}_\parallel^2 n_1(\mathbf{r}_S,t)]-\gamma\mathbf{u}(\mathbf{r}_S,t), \tag{2}$$

and Poisson's equation

$$\nabla^2\Phi(\mathbf{r},t)=4\pi[n_1(\mathbf{r}_S,t)\,\delta(\rho-a)-Q\,\delta(\mathbf{r}-\mathbf{r}_0)], \tag{3}$$

where Φ is the scalar potential which results from the external charge and the charge-density polarization of the electron gas, n_1. Note that, in Eqs. (1) and (2), $\boldsymbol{\nabla}_\parallel=\hat{\mathbf{e}}_z(\partial/\partial z)+a^{-1}\hat{\mathbf{e}}_\phi(\partial/\partial\phi)$ differentiates only tangentially to the nanotube surface [18], whereas in Eq. (3) the differentiation $\boldsymbol{\nabla}$ is unrestricted. The first term on the right-hand side of Eq. (2) is the force on electrons on the nanotube due to the tangential component of the electric field, the second and the third terms may be regarded as parts of the internal interaction force in the electron gas, while the last term, $-\gamma\mathbf{u}$, is the frictional force on electrons due to scattering on the positive-charge background, with γ being the friction coefficient. In particular, $\alpha=v_F^2/2$ is the speed of propagation of the density disturbances in the electron gas with $v_F=(2\pi n_0)^{1/2}$ being the Fermi velocity of the two-dimensional electron gas, whereas the choice $\beta=1/4$ in the term $(\beta/n_0)\boldsymbol{\nabla}_\parallel[\boldsymbol{\nabla}_\parallel^2 n_1(\mathbf{r},t)]$ in Eq. (2) describes single-electron excitations in the electron gas. We note that this term has been neglected in the work of Stöckli *et al.* [15], so that, as a consequence, a cutoff wave number had to be introduced to avoid the divergence of certain integrals.

It is convenient to consider separately the values of the total potential $\Phi=\Phi_1$ inside the nanotube ($\rho<a$) and $\Phi=\Phi_2$ outside the nanotube ($\rho>a$). The former part of the potential is composed of the potential Φ_0 due to the moving charged particle and the induced potential Φ_{ind} due to the charge polarization on the nanotube surface, so that $\Phi_1=\Phi_0+\Phi_{ind}$. Taking into account the natural boundary conditions at $\rho=0$ and $\rho=\infty$, these potential components can be expanded in terms of the cylindrical Bessel functions $I_m(x)$ and $K_m(x)$ [12,16,19], as follows:

$$\Phi_0(\rho,\phi,z,t)=\frac{Q}{|\mathbf{r}-\mathbf{r}_0|}=\frac{Q}{\pi}\sum_{m=-\infty}^{\infty}\int_{-\infty}^{\infty}dk e^{ik(z-vt)+im(\phi-\phi_0)}\times I_m(k\rho_<)K_m(k\rho_>), \tag{4}$$

where $\rho_<$ ($\rho_>$) is the smaller (larger) of ρ and ρ_0, and

$$\Phi_{ind}(\rho,\phi,z,t)=\frac{Q}{\pi}\sum_{m=-\infty}^{\infty}\int_{-\infty}^{\infty}dk e^{ik(z-vt)+im(\phi-\phi_0)}\times I_m(k\rho_0)I_m(k\rho)A_m(k). \tag{5}$$

Similarly, the total potential outside the nanotube ($\rho>a$) can be expanded as

$$\Phi_2(\rho,\phi,z,t)=\frac{Q}{\pi}\sum_{m=-\infty}^{\infty}\int_{-\infty}^{\infty}dk e^{ik(z-vt)+im(\phi-\phi_0)}\times I_m(k\rho_0)K_m(k\rho)B_m(k). \tag{6}$$

In order to simplify the notation, we adopt a convention that, whenever the momentum k appears in the argument of a Bessel function, it should be treated as the magnitude $|k|$, so that, e.g., $K_m(k\rho)\equiv K_m(|k|\rho)$, etc. [15]. The unknown coefficients A_m and B_m in Eqs. (5) and (6) can be determined by the following boundary conditions at $\rho=a$;

$$\Phi_1(\rho,\phi,z,t)\big|_{\rho=a}=\Phi_2(\rho,\phi,z,t)\big|_{\rho=a} \tag{7}$$

and

$$\left.\frac{\partial\Phi_2(\rho,\phi,z,t)}{\partial\rho}\right|_{\rho=a}-\left.\frac{\partial\Phi_1(\rho,\phi,z,t)}{\partial\rho}\right|_{\rho=a}=4\pi n_1(\phi,z,t). \tag{8}$$

Equation (8) means that, due to the polarization of the electron gas on the nanotube surface, the radial component of the electric field is discontinuous at the cylinder $\rho=a$. This boundary condition is different from that used in the studies of charged particles moving in cylindrical channels in solids [12–14,16], in which the radial component of the displacement field at the boundary is assumed to be continuous.

By eliminating the velocity field $\mathbf{u}(\mathbf{r},t)$, one obtains from Eqs. (1) and (2),

$$\left(\frac{\partial^2}{\partial t^2}+\gamma\frac{\partial}{\partial t}\right)n_1(\mathbf{r}_S,t)=-n_0\boldsymbol{\nabla}_\parallel^2\Phi(\mathbf{r},t)\big|_{\rho=a}+\alpha\nabla_\parallel^2 n_1(\mathbf{r}_S,t)-\beta\nabla_\parallel^2[\nabla_\parallel^2 n_1(\mathbf{r}_S,t)]. \tag{9}$$

According to the potential continuity condition, Eq. (7), $\Phi(\mathbf{r},t)$ appearing in Eq. (9) may be replaced by the potential $\Phi_2(\mathbf{r},t)$. Upon solving Eq. (9) by means of the space-time

Fourier-Bessel transform for the induced density on the cylindrical surface and using Eq. (8), we obtain

$$n_1(\phi,z,t)=\frac{Q}{\pi}n_0\sum_{m=-\infty}^{\infty}\int_{-\infty}^{\infty}dk e^{ik(z-vt)+im(\phi-\phi_0)} \times I_m(k\rho_0)C_m(k), \tag{10}$$

where

$$C_m(k)=-\frac{(k^2+m^2/a^2)K_m(ka)}{kv(kv+i\gamma)-\alpha(k^2+m^2/a^2)-\beta(k^2+m^2/a^2)^2} \times B_m(k). \tag{11}$$

Using Eqs. (4)–(6), (10), and (11) in Eqs. (7) and (8), it is easy to obtain the expressions for the coefficients A_m, B_m, and C_m, as follows:

$$A_m(k)=\frac{\Omega_p^2a^2(k^2+m^2/a^2)K_m^2(ka)}{kv(kv+i\gamma)-\omega_m^2(k)}, \tag{12}$$

$$B_m(k)=\frac{kv(kv+i\gamma)-\alpha(k^2+m^2/a^2)-\beta(k^2+m^2/a^2)^2}{kv(kv+i\gamma)-\omega_m^2(k)}, \tag{13}$$

$$C_m(k)=-\frac{(k^2+m^2/a^2)K_m(ka)}{kv(kv+i\gamma)-\omega_m^2(k)}, \tag{14}$$

where

$$\omega_m^2(k)=\alpha(k^2+m^2/a^2)+\beta(k^2+m^2/a^2)^2 +\Omega_p^2a^2(k^2+m^2/a^2)K_m(ka)I_m(ka) \tag{15}$$

with $\Omega_p=(4\pi n_0/a)^{1/2}$. One can see from Eqs. (12)–(14) that the resonant excitations will occur, in the case when the damping factor γ is zero, under the condition $kv=\omega_m(k)$. The resonant frequency $\omega_m(k)$ depends on the longitudinal wave number k, the angular momentum m, and the nanotube's radius a. Thus, we may calculate the induced potential and other relevant quantities by using the above expressions for the coefficients A_m, B_m, and C_m.

We study here the self-energy and the stopping power which represent the main effects of the induced electric field on a charged particle moving inside a carbon nanotube. Using the expression for the induced potential given in Eq. (5), we obtain the self-energy

$$E_{self}=\frac{1}{2}Q\Phi_{ind}(\mathbf{r},t)|_{\mathbf{r}=\mathbf{r}_0(t)} =\frac{Q^2}{\pi}\sum_{m=-\infty}^{\infty}\int_0^{\infty}dkI_m^2(k\rho_0)\mathrm{Re}\,A_m(k), \tag{16}$$

and the stopping power

$$S=Q\left.\frac{\partial\Phi_{ind}}{\partial z}\right|_{\mathbf{r}=\mathbf{r}_0(t)} =-\frac{2Q^2}{\pi}\sum_{m=-\infty}^{\infty}\int_0^{\infty}dkkI_m^2(k\rho_0)\mathrm{Im}\,A_m(k). \tag{17}$$

In particular, the integration in Eq. (17) may be carried out for infinitesimally small damping ($\gamma\to 0^+$), giving

$$S=2Q^2\Omega_p^2\sum_{m=-\infty}^{\infty}k_m[(k_ma)^2+m^2]I_m^2(k_m\rho_0)K_m^2(k_ma) \times\left|\frac{\partial Z_m(k)}{\partial k}\right|^{-1}_{k=k_m}, \tag{18}$$

where $Z_m(k)=(kv)^2-\omega_m^2(k)$ and k_m is determined by the condition of the plasma resonance, $(k_mv)^2=\omega_m^2(k_m)$.

In the following calculations, we consider the charged particle to be proton, $Q=1$, and assume that the surface electron density of a single-wall carbon nanotube can be approximated by the electron-gas density of a graphite sheet, $n_0=4\times 0.107$ [20]. Figures 1(a) and 1(b) show the influence of the damping factor γ on the velocity dependence of the self-energy and the stopping power, respectively, for charged particles moving along the axis ($\rho_0=0$) of a nanotube with the radius $a=20$. It is clear that the magnitudes of both the self-energy and the stopping power decrease with increasing γ values. In addition, we observe that, with the increasing γ values, the regions where the self-energy is negative, as well as the peaks of the stopping power, shift to lower velocities. Similar behavior has been found in the case of particles moving inside cylindrical channels in solids [13].

Whereas the physical origin of damping lies in the momentum losses of excited electrons during their scattering on ion cores on the nanotube, the damping constant γ may be also used as a phenomenological factor taking into account the broadening of the plasmon resonance in excitation spectra of various materials [13]. In the present context, finite value of γ also provides a mathematical convenience in executing the integral in Eq. (16) which contains a (removable) singularity when $\gamma=0$. Thus, while the curve labeled by $\gamma/\Omega_p=0$ in Fig. 1(b) has been easily calculated from Eq. (18) for stopping power, we have tested very small values of $\gamma/\Omega_p=0.0005$ and 0.001 in Eq. (16) for self-energy and obtained the corresponding curves in Fig. 1(a), showing that $\gamma/\Omega_p=0.001$ may be considered practically zero in the subsequent calculations, while rendering the integral in Eq. (16) nonsingular. In passing, we note that the results with finite γ in Fig. 1 should be taken with some discretion, since it is known that phenomenological damping may lead to violation of the oscillator-strength sum rule, related to the conservation of electrons. This problem can be, in principle, regulated by using Mermin's approach [21] for a dielectric function, but we do not pursue the issue any further here and regard the curves with finite γ in Fig. 1 only as qualitative description of possible effects of damping.

In Figs. 2(a) and 2(b), we show the self-energy and the stopping power versus the charged particle's velocity v, for

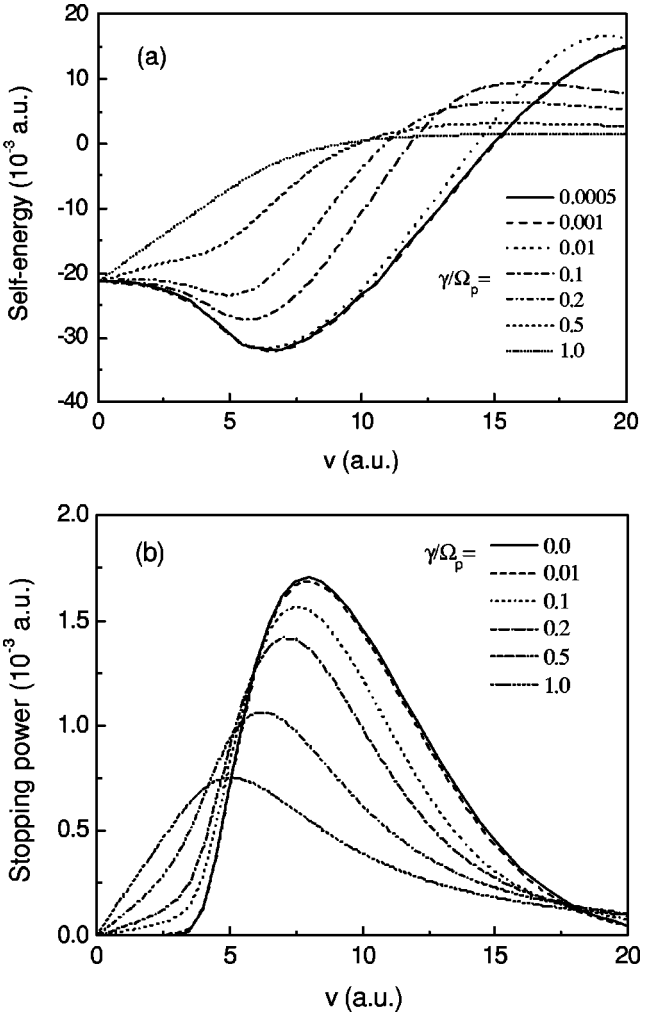

FIG. 1. Effects of the damping factor γ on the velocity dependence of (a) the self-energy and (b) the stopping power, for a proton moving in a carbon nanotube with $a=20$ a.u. and $\rho_0=0$.

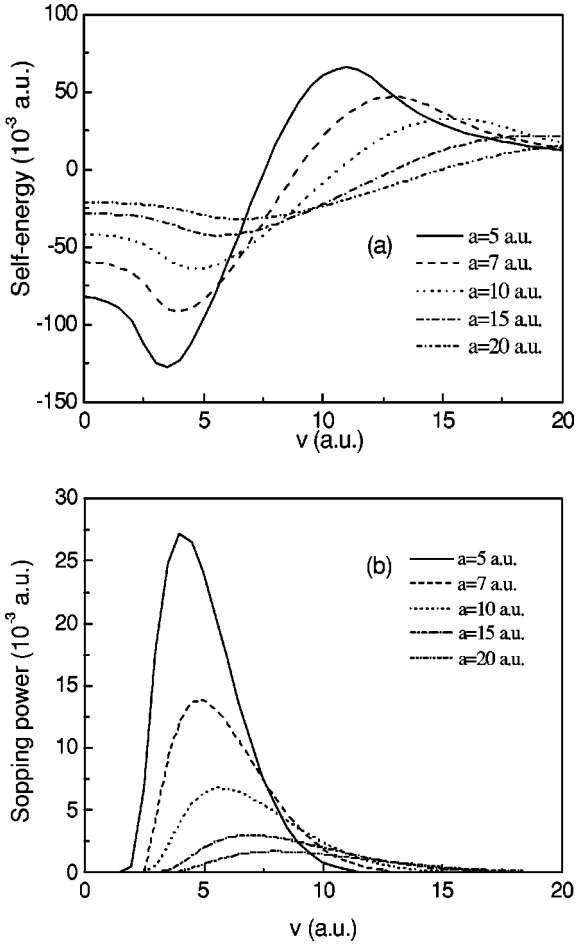

FIG. 2. Effects of the nanotube radius a on the velocity dependence of (a) the self-energy with $\gamma=0.001\,\Omega_p$, and (b) the stopping power with $\gamma=0$, for a proton moving in a carbon nanotube at $\rho_0=0$.

several values of the radius a of the nanotube, with the particle position being $\rho_0=0$ and with zero damping. One observes that, when the radius a increases, not only the self-energy and the stopping power decrease in magnitude, but also their extrema move to higher velocities.

The influence of the charged particle position ρ_0 on the dependence of the self-energy and the energy loss on velocity are shown in Figs. 3(a) and 3(b), for $a=20$ and with zero damping. For a fixed velocity, both the self-energy and the stopping power have the smallest magnitude when the particle moves along the nanotube axis, and increase in magnitude when the particle position shifts closer to the surface of the nanotube. One also observes that the positions of extrema in both sets of curves shift to lower velocities as the particle position moves closer to the wall of the nanotube.

III. COMPARISON WITH RPA DIELECTRIC FORMALISM

The simplest way to calculate the induced potential, Eq. (5), by means of the longitudinal dielectric function in RPA for 2D electron gas on the cylindrical surface of a nanotube [17], $\epsilon(\mathbf{r}_S-\mathbf{r}'_S,t-t')=\epsilon(\phi-\phi',z-z',t-t')$, is to use the *constitutive equation* approach of Stern [22] for the tangential components of the displacement field at the nanotube surface, $\mathbf{D}_\parallel$, which is related to the external potential Φ_0 via

$$\mathbf{D}_\parallel(\phi,z,t)\equiv-\boldsymbol{\nabla}_\parallel\Phi_0(a,\phi,z,t), \tag{19}$$

and the total electric field at the nanotube surface, $\mathbf{E}_\parallel$, related to the value of the total potential at the nanotube surface, $\Phi_1=\Phi_2$, cf Eq. (7), by

$$\mathbf{E}_\parallel(\phi,z,t)\equiv-\boldsymbol{\nabla}_\parallel\Phi_2(a,\phi,z,t). \tag{20}$$

Since the longitudinal dielectric function for the nanotube is diagonal [17] in the Fourier-Bessel representation (k,m), the constitutive equation simply reads

$$\mathbf{D}_\parallel(k,m,\omega)=\epsilon(k,m,\omega)\,\mathbf{E}_\parallel(k,m,\omega), \tag{21}$$

so that, after using Eqs. (4) and (6) in Eqs.(19)–(21), we obtain

$$I_m(k\rho_0)\,K_m(ka)=\epsilon(k,m,kv)I_m(k\rho_0)\,K_m(ka)\,B_m(k), \tag{22}$$

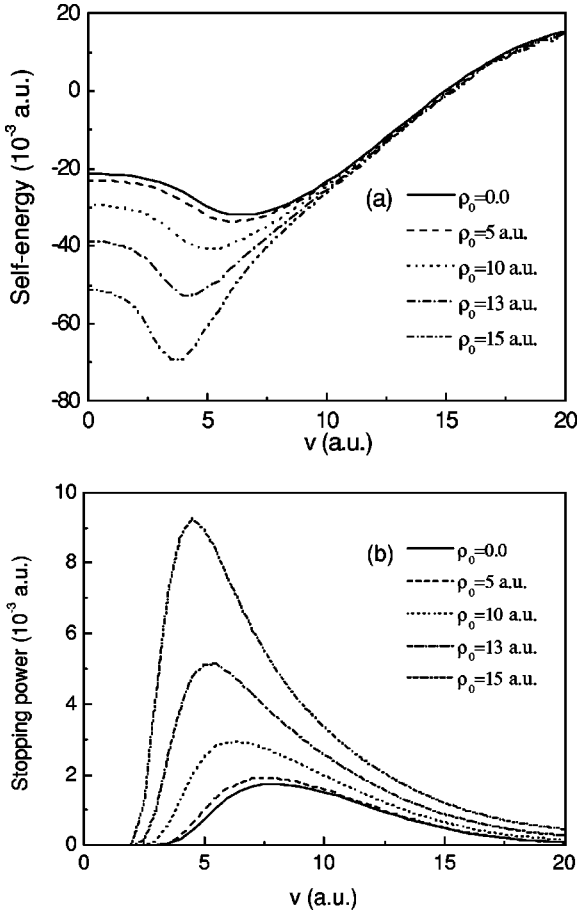

FIG. 3. Effects of the particle position ρ_0 on the velocity dependence of (a) the self-energy with $\gamma=0.001\,\Omega_p$, and (b) the stopping power with $\gamma=0$, for a proton moving in a carbon nanotube with $a=20$ a.u.

and consequently

$$B_m(k)=\epsilon^{-1}(k,m,kv). \tag{23}$$

Since the condition, Eq. (7), gives

$$I_m(k\rho_0)\,K_m(ka)+I_m(k\rho_0)\,I_m(ka)\,A_m(k) = I_m(k\rho_0)\,K_m(ka)\,B_m(k), \tag{24}$$

we finally obtain

$$A_m(k)=\frac{K_m(ka)}{I_m(ka)}[\epsilon^{-1}(k,m,kv)-1], \tag{25}$$

which is to be used in Eq. (17) to evaluate the stopping power in the RPA dielectric function approach. We note that the result obtained in this way is different and somewhat simpler than the result obtained for stopping power in our previous paper [16]. Namely, the boundary conditions used in Ref. [16] are not really appropriate for an isolated nanotube, but are more appropriate for determining the dielectric response of a nanotube in a bundle or a rope of carbon nanotubes, similar to a nanochannel in a solid [12–14], whereas the boundary conditions, Eqs. (22) and (24), are strictly appropriate for an isolated single-wall carbon nanotube in free space. We finally remark that the boundary condition, Eq. (8), is not required for calculation of the induced potential in 3D space when the dielectric function for the 2D electron gas is used, but is rather replaced with the constituent equation (21) giving the condition, Eq. (22). Of course, the condition, Eq. (8), is still valid, and may be used to, e.g., calculate the induced charge density on the nanotube, n_1, once the values of the potential, Φ_1 and Φ_2, are determined on each side of the nanotube surface.

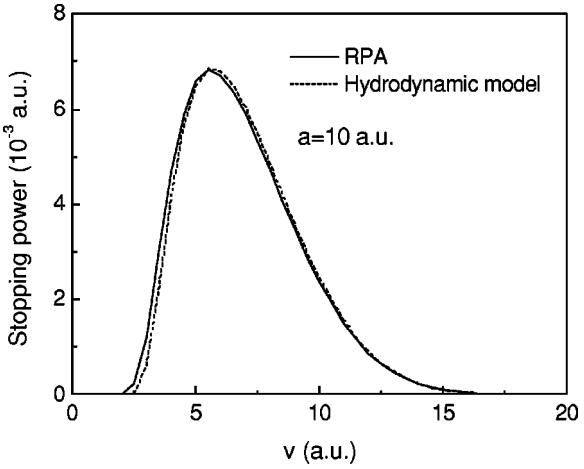

FIG. 4. Comparison of the velocity dependence of stopping power calculated by the hydrodynamic model with that calculated from the dielectric formalism in the RPA, for a proton moving at $\rho_0=0$ in a nanotube with $a=10$ a.u. and $\gamma=0$.

Since we are interested here in energy losses of charged particles moving at high speeds through nanotubes, which are dominated by the collective excitations of the 2D electron gas, we calculate the stopping power in the RPA dielectric approach, given by Eq. (17) with Eq. (25), under the resonance condition, $\mathrm{Im}\,\epsilon(k,m,kv)=0$ [12,13,16]. This result is compared in Fig. 4 with the stopping power obtained from the hydrodynamic theory of the previous section for proton moving at $\rho_0=0$ through a nanotube with radius $a=10$ and $\gamma=0$. The two curves in Fig. 4 appear to be very close, except for lower speeds, indicating that the hydrodynamic model may be considered as a very good and rather simple approximation to the RPA dielectric approach, at least when the energy losses of fast charges are concerned.

IV. CONCLUDING REMARKS

We have used the linearized hydrodynamic model in conjunction with the Poisson equation to describe the electronic excitations of the 2D electron gas confined on surfaces of nanotubes. General expressions have been derived for the induced potential, the self-energy, and the stopping power for charged particles moving parallel to the axis in carbon nanotubes. The numerical results show that the velocity dependences of these quantities are strongly affected by the damping factor, the nanotube radius, and the particle position. From a comparison of the calculations of the stopping power in the hydrodynamic model with those based on the dielec-

tric function in RPA, we find a fairly good agreement between the two approaches, indicating that the hydrodynamic model is a very good approximation to the RPA approach for energy losses of fast charges, which are dominated by the collective excitations. On the other hand, the approach based on the dielectric function in RPA should be considered more reliable in describing the single-electron excitations, which give important contribution to the energy losses at lower speeds [16].

Since the particle self-energy mainly arises from virtual excitations of the nanotube-surface collective modes, it is expected that the hydrodynamic model also provides an adequate description of the self-energy of fast charges moving through nanotubes. In particular, we have shown that the self-energy of a fast charged particle takes increasingly large negative values as the particle moves away from the center of a nanotube, reaching the value of a fraction of eV close to the surface of the nanotube. This implies that there should exist a strong transverse force deflecting particles transported through nanotubes toward the nanotube walls. We note that several authors [4–8] have presented computer simulations of the charged-particle propagation through nanotubes, where neither the longitudinal stopping force nor the transverse deflection force due to the electronic excitations were taken into account. We believe that the results obtained in the present work may be readily used in future simulations of the transport of charged particles through nanotubes to include the energy losses and the effects of the self-energy on the particle trajectories.

ACKNOWLEDGMENTS

This work was jointly supported by the National Natural Science Foundation of China (Grant No. 10275009) and the Ministry of Education State of China (Y.N.W.). Z.L.M. acknowledges the support by the Natural Sciences and Engineering Research Council of Canada.

[1] A. Rivacoba, P. Appell, and N. Zabala, Nucl. Instrum. Methods Phys. Res. B **96**, 465 (1995).
[2] T. Pichler, M. Knupfer, M.S. Golden, and J. Fink, Phys. Rev. Lett. **80**, 4729 (1998).
[3] M. Knupfer *et al.*, Carbon **37**, 733 (1999).
[4] N.K. Zhevago and V.I. Glebov, Phys. Lett. A **310**, 301 (2003).
[5] N.K. Zhevago and V.I. Glebov, Phys. Lett. A **250**, 360 (1998).
[6] S. Bellucci *et al.*, Nucl. Instrum. Methods Phys. Res. B **202**, 236 (2003).
[7] G.V. Dedkov, Nucl. Instrum. Methods Phys. Res. B **143**, 584 (1998).
[8] L.A. Gevorgian, K.A. Ispirian, and R.K. Ispirian, Nucl. Instrum. Methods Phys. Res. B **145**, 155 (1998).
[9] J. Crowell and R.H. Ritchie, Phys. Rev. **172**, 436 (1968); D.P. Spears, J.D. Allen, V.E. Anderson, R.S. Becker, H.H. Hubbell, T.L. Ferrel, R.H. Ritchie, and R.D. Birkhoff, J. Appl. Phys. **50**, 3039 (1979); R.S. Becker, V.E. Anderson, R.D. Birkhoff, T.L. Ferrel, and R.H. Ritchie, Can. J. Phys. **59**, 521 (1981).
[10] K. Tőkési, L. Wirtz, and J. Burgdörfer, Nucl. Instrum. Methods Phys. Res. B **154**, 307 (1999).
[11] K. Tőkési, L. Wirtz, C. Lemell, and J. Burgdörfer, Nucl. Instrum. Methods Phys. Res. B **164**, 504 (2000).
[12] N.R. Arista and M.A. Fuentes, Phys. Rev. B **63**, 165401 (2001).
[13] N.R. Arista, Phys. Rev. A **64**, 032901 (2001).
[14] N.R. Arista, Nucl. Instrum. Methods Phys. Res. B **182**, 109 (2001).
[15] T. Stöckli, J.M. Bonard, A. Châtelain, Z.L. Wang, and P. Stadelmann, Phys. Rev. B **64**, 115424 (2001).
[16] Y.N. Wang and Z.L. Mišković, Phys. Rev. A **66**, 042904 (2002).
[17] M.F. Lin and K.W.-K. Shung, Phys. Rev. B **47**, 6617 (1993).
[18] G. Barton and C. Eberlein, J. Chem. Phys. **95**, 1521 (1991).
[19] J. D. Jackson, *Classical Electrodynamics* (Wiley, New York, 1975).
[20] D. Ostling, D. Tomanek, and A. Rosen, Phys. Rev. B **55**, 13 980 (1997).
[21] N.D. Mermin, Phys. Rev. B **1**, 2362 (1970).
[22] F. Stern, Phys. Rev. Lett. **18**, 546 (1967).